RSC Mechanochemistry

ROYAL SOCIETY OF CHEMISTRY

PAPER

View Article Online
View Journal | View Issue

Cite this: *RSC Mechanochem.*, 2025, **2**, 584

Preparation of lead dodecyl sulfate nanorod materials mediated by mechanochemistry and green solvent-free catalytic synthesis of heterocyclic derivatives†

Zhiqiang Wu, ‡*[ab] Yuan Min,‡[b] Yongqin Li,[b] Fang Qian,[b] Lin-an Cao,[b] Rong Tan,[c] Enke Feng,[b] Jiya Ding*[b] and Pengxi Jiang[d]

Received 25th October 2024
Accepted 4th May 2025

DOI: 10.1039/d4mr00123k

rsc.li/RSCMechanochem

In this work, the lead dodecyl sulfate material ($Pb(DS)_2$) was successfully synthesized for the first time *via* a mechanochemical ball milling method. The synthesized material was comprehensively analyzed using scanning electron microscopy (SEM), high-resolution transmission electron microscopy (HRTEM), Fourier transform infrared (FT-IR) spectroscopy, X-ray diffraction (XRD), thermogravimetric analysis (TGA), X-ray photoelectron spectroscopy (XPS) and nuclear magnetic resonance (NMR) spectroscopy. The results demonstrate that the $Pb(DS)_2$ catalyst, synthesized *via* solvent-free mechanical ball milling, possesses a distinctive solid nanorod morphology. Furthermore, the catalyst efficiently promotes the synthesis of heterocyclic derivatives in a solvent-free environment within 20 minutes, achieving a target product yield of up to 98%. Specifically, it produced bis(indolyl)methane derivatives with yields ranging from 78% to 98%, and quinoxaline derivatives with yields ranging from 87% to 98% within the same timeframe. The $Pb(DS)_2$ catalyst also exhibits remarkable catalytic activity in the Biginelli reaction. Notably, the catalyst maintains excellent and stable performance over eight recycling cycles.

Introduction

In recent years, mechanochemistry has emerged as one of the most promising alternatives to traditional liquid-phase reactions, owing to its solvent-free and environmentally friendly nature. This approach has revolutionized various fields of chemistry,[1,2] showcasing epoch-making significance. Mechanochemistry utilizes mechanical energy to drive physical and chemical transformations, enabling the design of complex molecules and nanostructured materials. Additionally, it enhances the dispersion and recombination of multiphase components, while accelerating reaction rates and efficiencies by generating highly reactive surfaces. In addition to their efficiency and practicality, mechanochemical reactions are distinguished by their occurrence in the solid state without the need for bulk solvents, making them inherently solvent-free.[3,4] The mechanochemical synthesis method offers numerous advantages, including shortened reaction times, clean and safe reaction conditions, high product yields, minimal or no use of organic solvents, and distinct product selectivity. The mechanochemical synthesis method demonstrates multiple advantages over traditional synthesis processes, mainly reflected in the following three dimensions: first, in terms of reaction efficiency, this method can significantly shorten the reaction time and increase the product yield; second, in terms of environmental friendliness, its reaction process has the characteristics of being clean and safe, and can effectively reduce or completely avoid the use of organic solvents, which conforms to the principles of green chemistry. Finally, in terms of product control capability, this technology can achieve precise control of product selectivity through mechanical force regulation. This multi-dimensional advantage gives it significant application value in the field of sustainable chemical synthesis.[5] Mechanochemical synthesis has emerged as a viable alternative for green chemical processes, particularly in organic synthesis,[6–9] coordination polymer chemistry,[10–12] and the development of metal–organic frameworks (MOFs),[13] among others. The rapid development of mechanochemical synthesis provides a simple, efficient, economical and environmentally friendly approach for preparing solid catalysts, demonstrating broad application

[a]*School of Civil and Hydraulic Engineering, Ningxia University, Yinchuan, 750021, P. R. China*

[b]*Ningxia Key Laboratory of Green Catalytic Materials and Technology, College of Chemistry and Chemical Engineering, Ningxia Normal University, Guyuan, 756099, P. R. China. E-mail: wuzqns@nxnu.edu.cn*

[c]*College of Chemistry and Chemical Engineering, Hunan Normal University, Changsha, 410081, P. R. China*

[d]*Inner Mongolia Bairun Technology Co., Ltd., Alxa League, Inner Mongolia, 750300, P. R. China*

† Electronic supplementary information (ESI) available. See DOI: https://doi.org/10.1039/d4mr00123k

‡ Zhiqiang Wu and Yuan Min contributed equally to this work.

prospects.[14] Multi component reactions (MCRs) are important tools for constructing complex molecules in organic synthesis, capable of forming multiple chemical bonds in a one pot process.[15–17] Heterogeneous catalysts have attracted much attention for their improved reaction efficiency and selectivity in MCRs. These catalysts can promote coupling between different reactants, generating compounds with biological activity and industrial application value.

Nitrogen-containing heterocyclic compounds have gained significant importance in pharmaceuticals and bioactive natural products over the last decade. Notably, bis(indolyl) methanes and quinoxalines have demonstrated substantial pharmacological relevance due to their diverse biological activities. Various types of catalysts have been used to synthesize these derivatives, including $Ru_3(CO)_{12}$/$CsOH\cdot H_2O$,[18] silica gel,[19] $Ni(OTf)_2$,[20] ^{t}BuONa/DMSO,[21] Ni@Co_3O_4,[22] TCCA,[23] ionic liquids,[24] *etc.*[25,26] However, many of these methods are hindered by issues such as expensive catalysts, the use of toxic solvents, prolonged reaction times, complex post-processing procedures, and difficulties in catalyst recycling. Consequently, there is a pressing need to develop a straightforward, cost-effective, safe, and environmentally friendly approach for synthesizing N-containing heterocyclic compounds. Lead metal has a wide range of applications in the field of organic synthesis, especially in the synthesis of specific organic compounds.[27] Its excellent physical and chemical properties make it a common element in chemical laboratories.[28–31] Lead based catalysts exhibit excellent catalytic performance in oxidation and reduction reactions. For example, nano-β-lead dioxide catalysts can be used for photocatalytic CO_2 reduction, converting CO_2 into high-value C_{2+} chemicals.[32] Similarly, in organic coupling reactions, lead based catalysts can promote the reaction and generate the target product. For example, lead catalysts can be used for photocatalytic α-alkylation reactions to achieve C–C bond formation of aldehydes.[33] Although lead itself has certain toxicity, lead catalysts can play an important role in specific green chemistry processes through rational design and use. For example, in some photocatalytic reactions, lead catalysts can achieve efficient organic synthesis under mild conditions, reducing environmental impact.[32]

In the late 1990s, Kobayashi *et al.* pioneered the development and investigation of Lewis acid surfactant combination catalysts (LASCs; the catalysts mainly include $Sc(DS)_3$, $Fe(DS)_3$, $Zr(DS)_4$, *etc.*) in aqueous organic catalytic synthesis, including Fourier alkylation, Michael addition, allylation reactions, and even other asymmetric reaction types, all of which achieved ideal catalytic effects.[34–39] Wu *et al.* utilized $Sc(DS)_3$ to synthesize Friedländer quinoline derivatives from 2-aminobenzophenone and fatty aldehydes in an aqueous medium at 40 °C, with a yield of over 90% for the target products.[40] Zolfigol *et al.* employed $Zr(DS)_4$ to facilitate the reaction of indole with aldehydes or ketones at room temperature in an aqueous system, achieving positive outcomes. Despite the catalyst maintaining repeated catalytic performance after multiple centrifugation operations, it had a shorter cycle life.[41] Subsequently, Shekouhy *et al.* also used $Zr(DS)_4$ to efficiently synthesize a series of quinoline derivatives by catalyzing the reaction between 2-aminobenzamide and carbonyl compounds at room temperature within a short timeframe.[42] Ollevier *et al.* utilized the $Fe(DS)_2$ catalyst system to carry out the Mukaiyama aldol reaction in an aqueous phase, achieving excellent results with high enantioselectivity (ER value of 98 : 2).[43] Furthermore, Singh *et al.* advanced the field by developing $Fe(DS)_3$ catalysts for the efficient synthesis of quinoxaline compounds in the aqueous phase.[44] Additionally, Veisi *et al.* investigated the synthesis of bis(indolyl)methanes catalyzed by $Fe(DS)_3$ in water.[45] The synthesis method of the LASC catalyst system is simple and rapid, effectively addressing the issues of Lewis acid decomposition in water and the inherent incompatibility between organic matter and water. However, there are still significant challenges in the regeneration application of catalysts and the use of demulsifiers in post-treatment processes, which can lead to the generation of large amounts of toxic metal and surfactant organic wastewater (approximately 350 mL of SDS toxic wastewater is generated for every 2.74 mmol of LASC catalyst prepared). The utilization of mechanochemical methods not only mitigates wastewater generation but also enhances product yield, improves catalyst reusability, and addresses some of the limitations associated with the LASC catalyst. The mechanochemical method demonstrates multi-dimensional collaborative advantages: first, in the dimension of environmental benefits, it effectively reduces wastewater discharge through solid-state reaction mechanisms and significantly improves atomic economy; second, at the level of process optimization, it simultaneously increases the product yield and the recycling rate of the catalyst to achieve efficient resource utilization. What is more worthy of attention is that in terms of catalytic system innovation, the inherent limitations of coordination unsaturated site catalysts (LASCs) have been broken through, successfully solving key problems such as the easy inactivation of active sites and the difficulty in regulating reaction selectivity. The coupling effect of this triple advantage provides a new technical path for the development of green chemical processes. Furthermore, our group has recently developed a mechanochemical synthesis method for preparing the $La(DS)_3$ catalyst and has comprehensively investigated its structural and physicochemical properties. Additionally, a series of organic small molecule products were synthesized *via* solvent-free grinding, yielding promising results.[46]

Based on this, the preparation of Lewis acid composite catalysts *via* mechanochemical grinding under solvent-free conditions and their application in solvent-free solid-state grinding reactions show significant potential. Mechanochemistry plays a pivotal role in advancing green chemistry by restricting or effectively reducing the generation of pollutants from the source. In this work, we successfully synthesized the $Pb(DS)_2$ catalyst using mechanochemical methods for the first time and applied it to the synthesis of bis(indolyl)methane and quinoxaline derivatives under solvent-free conditions. The catalyst offers several advantages, including simple preparation, solvent-free reactions, and short grinding times. In addition, it is noteworthy that the $Pb(DS)_2$ catalyst exhibits an efficient cyclic service life, with experimental results indicating negligible loss of the Pb element. This not only maintains the

catalyst's activity but also prevents environmental contamination from heavy metals.

Results and discussion

Characterization of the $Pb(DS)_2$ catalyst

The experiment included a comprehensive structural characterization of the $Pb(DS)_2$ catalyst to gain deeper insights into its catalytic performance. The morphology and structure of the catalyst are illustrated in Fig. 1. It is noteworthy that the $Pb(DS)_2$ catalyst, prepared using a solvent-free mechanochemical ball milling method at room temperature, displayed a uniform nanorod-like structure without distinct pore distribution, as depicted in Fig. 1b. In contrast, pure lead nitrate exhibited an irregular nanorod-like morphology, as shown in Fig. 1a. High-resolution transmission electron microscopy (HRTEM) analysis revealed that the $Pb(DS)_2$ catalyst possessed a solid nanorod shape with a diameter ranging from approximately 2.5 to 3.0 nm (Fig. 1c). This unique morphology may be attributed to the structural reorganization of lead nitrate and SDS under mechanical force, as well as the double-layer linear arrangement of SDS molecules in a head to head and tail to tail configuration. The formation of nanorod-like materials may be influenced by mechanical stress, and special nanorod like or nanosheet layer materials may be more conducive to electron mass transfer and transmission, which will effectively improve the catalytic performance of the material.[47] The selected area electron diffraction (SAED) pattern revealed three concentric rings with diffraction radii of ~3.45 nm, ~1.71 nm and ~1.15 nm corresponding to the (001), (002) and (003) planes of $Pb(DS)_2$, respectively (as shown in Fig. 1d). Although the crystallinity of catalyst $Pb(DS)_2$ is not high, the presence of diffraction concentric rings still confirms the existence of $Pb(DS)_2$. The XRD characterization results also confirmed the above conclusion (Fig. 2a). Compared with the SDS sample, the XRD diffraction peaks of the $Pb(DS)_2$ catalyst were significantly weaker and broader, indicating a certain degree of decrease in its crystallinity. In this work, it was demonstrated for the first time that $Pb(DS)_2$ nanorod-like composite materials synthesized by mechanical ball milling exhibit superior catalytic performance in several representative organic synthesis reactions (as shown in Tables 2 and 3). Energy dispersive X-ray spectroscopy (EDS mapping) verified the presence of C, O, S, and Pb elements within the $Pb(DS)_2$ catalyst.

The structural characterization of the $Pb(DS)_2$ catalyst was conducted using X-ray diffraction (XRD) analysis, as shown in Fig. 2a. In the low-angle region of the X-ray powder diffractograms, three strong reflections were observed, with the peak at the lowest angle exhibiting the highest intensity for the catalyst. The solid displayed a moderate degree of crystallinity, as evidenced by the relatively broad diffraction peaks observed in the low θ region. According to Bragg's law ($n_\lambda = 2d \sin\theta$, where θ is the diffraction half angle and λ is the wavelength of the incident wave), SDS exhibited three distinct sharp diffraction peaks at 3.98 nm, 2.00 nm, and 1.34 nm, respectively, while $Pb(DS)_2$ also displayed three different diffraction peaks with intensities of 3.48 nm, 1.72 nm, and 1.14 nm, respectively. It is worth noting that compared to SDS, all three diffraction peaks in the $Pb(DS)_2$ catalyst exhibit a significant red shift towards longer wavelengths. Furthermore, the diffraction peaks of the catalyst are relatively broader, indicating a certain degree of reduction in

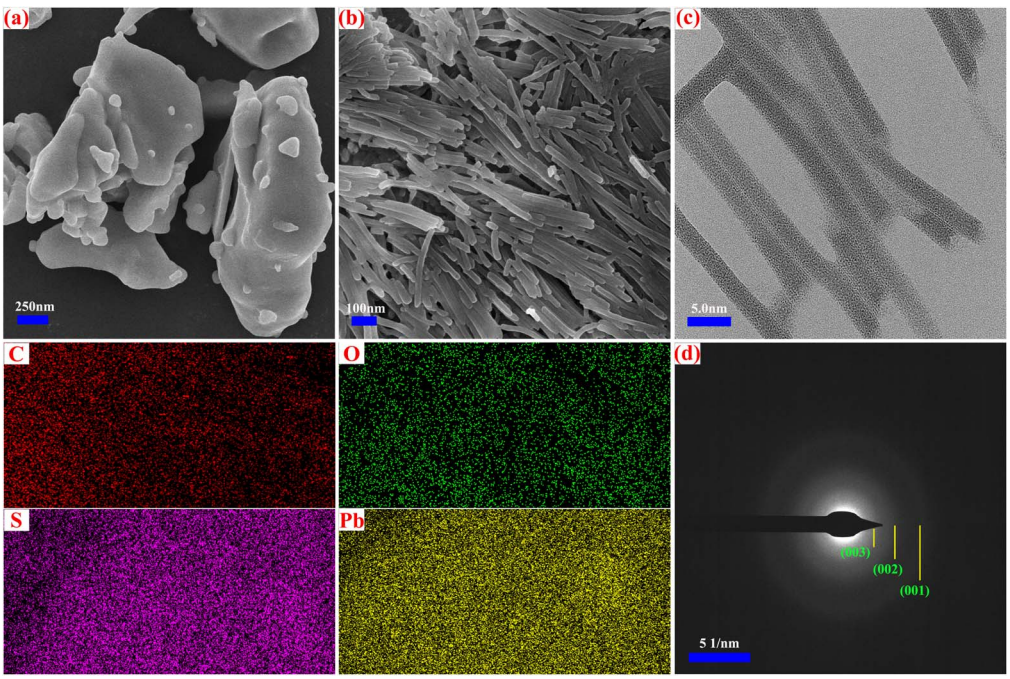

Fig. 1 SEM images of (a) $Pb(NO_3)_2$ and (b) $Pb(DS)_2$, HRTEM images of (c) $Pb(DS)_2$, and the SAED pattern of (d) $Pb(DS)_2$, including EDS mapping spectra.

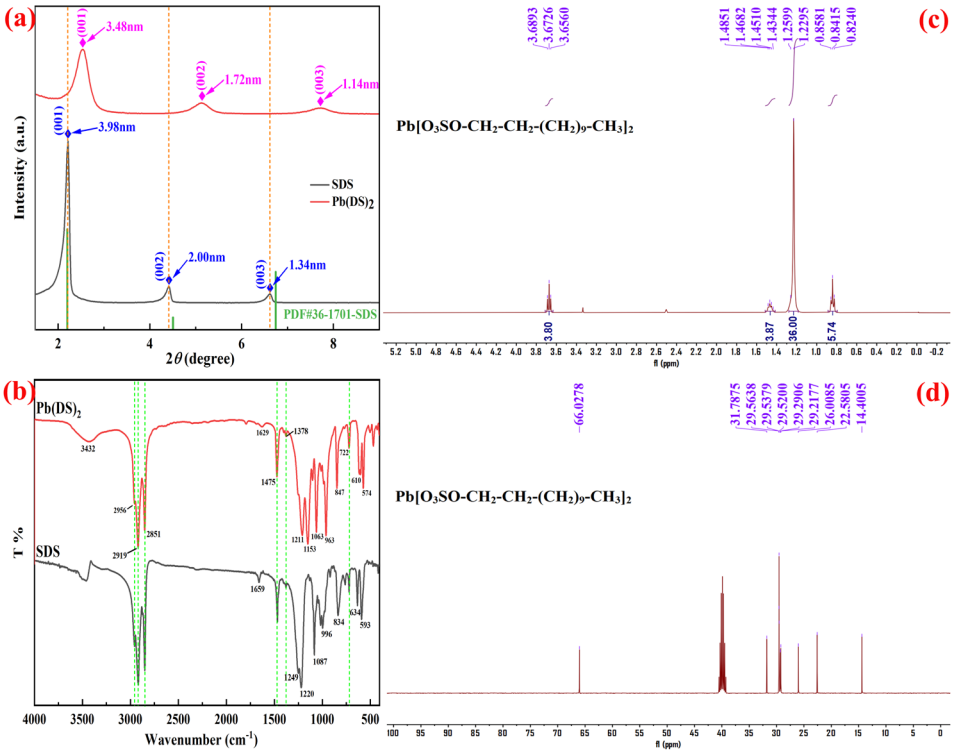

Fig. 2 The XRD (a), FT-IR (b), ^{1}H-NMR (c), and ^{13}C-NMR (d) spectra of $Pb(DS)_2$, respectively.

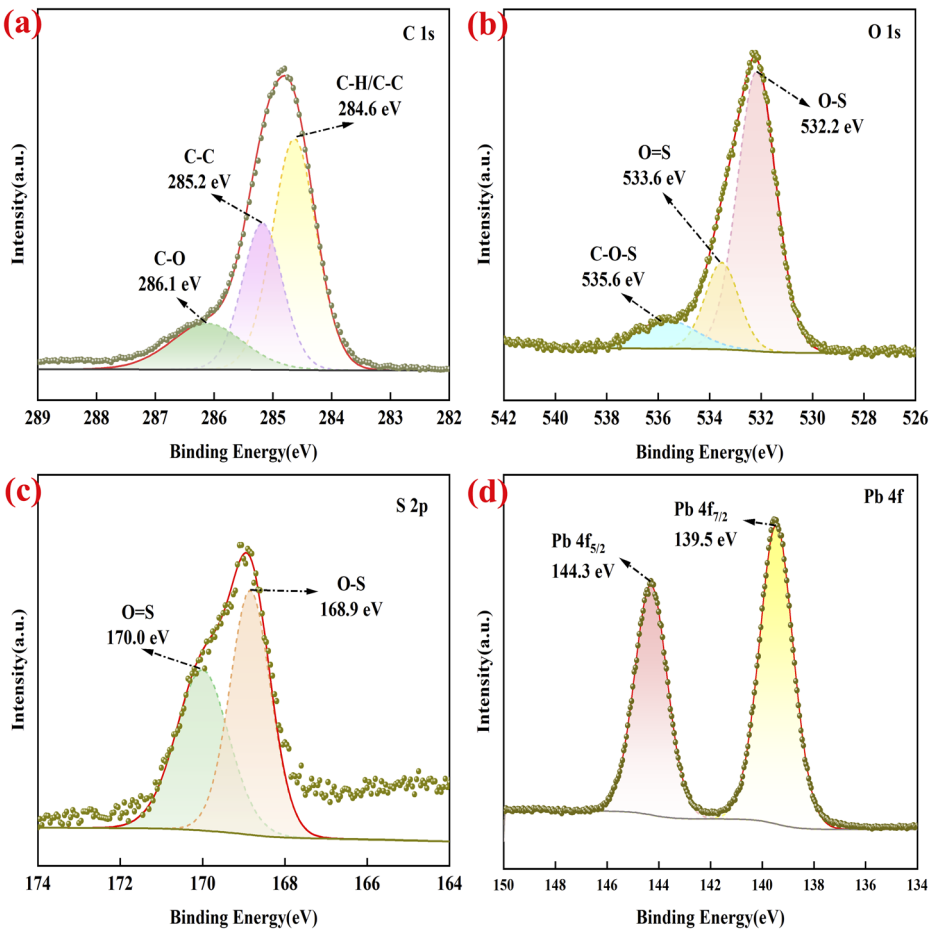

Fig. 3 The XPS of the $Pb(DS)_2$ catalyst.

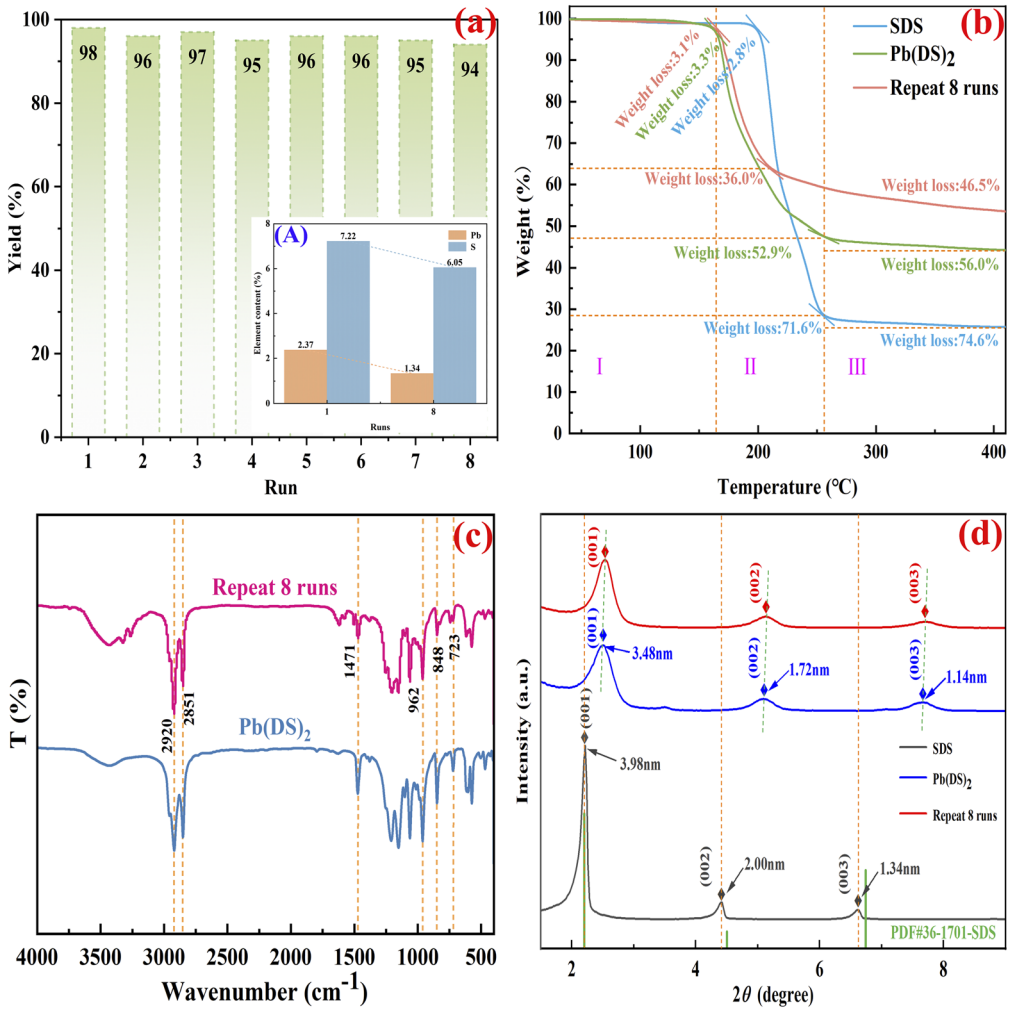

Fig. 4 The experimental evaluation of $Pb(DS)_2$ recycling (a), elemental analysis of the fresh $Pb(DS)_2$ catalyst and after 8 runs (A), TGA (b), FT-IR (c) and XRD (d), respectively.

the crystallinity of the $Pb(DS)_2$ catalyst compared to SDS, which is consistent with the SAED analysis mentioned above.

Fig. 2b shows the FT-IR spectra of SDS and the $Pb(DS)_2$ catalyst. The spectrum of the $Pb(DS)_2$ catalyst displays characteristic bands corresponding to: (i) stretching and bending vibration modes of the alkyl chain, with similar positions and relative intensities, such as 2919 cm^{-1} and 1378 cm^{-1} representing the bending and stretching vibrations of $-CH_3$, and 2851 cm^{-1} and 1475 cm^{-1} representing the bending and stretching vibrations of $-CH_2$;[48] and (ii) stretching and bending vibration modes of the anionic headgroup at 463 cm^{-1} (symmetric OSO_3–bending); 574 cm^{-1} and 610 cm^{-1} (degenerate asymmetric OSO_3–bending); 847 cm^{-1} (symmetric S–OC stretching); 963 cm^{-1} (asymmetric S–OC stretching); 1063 cm^{-1} and 1107 cm^{-1} (degenerate symmetric OSO_3-stretching); and 1211 cm^{-1} and 1153 cm^{-1} (asymmetric OSO_3-stretching).[49] The significant shifts and splittings of both symmetric and asymmetric modes, compared to the SDS spectrum, were attributed to the interaction between dodecylsulfate anions and Pb(II) cations.[50] Consequently, the local geometry of the OSO_3 site is highly asymmetric and close to C_{2v} symmetry.[51] The headgroup region is particularly sensitive to changes induced by positively charged species.[52] The spectrum of SDS closely resembled that reported by Sperline[53] for the $SDS_{1/8}$ hydrate material, where only a minor splitting of the OSO_3 group was observed (C_{3v} symmetry[51]). The catalyst was characterized by ^{1}H-NMR, revealing chemical shifts at $d = 0.84$ ppm (triplet, 6H, and $J = 6.82$ Hz); 1.26 ppm (m, 36H); 1.46 ppm (m, 4H); and 3.67 ppm (triplet, 4H, and $J = 6.66$ Hz) in DMSO (Fig. 2c). In the DMSO solvent, the water signal at $d = 3.37$ ppm is attributed to the H_2O molecules from the catalyst and solvent. The ^{13}C-NMR spectrum of $Pb(DS)_2$ in DMSO shows characteristic peaks of dodecylsulfate compounds at $d = 14.40$, 22.58, 26.00, 29.22, 29.52, 29.54, 29.56, 31.79, and 66.03 ppm (Fig. 2d). The SEM analysis (Fig. 1b) clearly indicates that the $Pb(DS)_2$ catalyst has a distinct nanofiber rod-shaped structure.

The X-ray photoelectron spectroscopy (XPS) analysis was employed to investigate the chemical state and valence of the elements in $Pb(DS)_2$, as shown in Fig. 3. The narrow scans of C 1s, O 1s, S 2p, and Pb 4f were deconvoluted to investigate the bonding information of each element in detail. The XPS spectrum of C 1s (Fig. 3a) exhibited binding energy peaks at

Table 1 The optimization of reaction conditions[d]

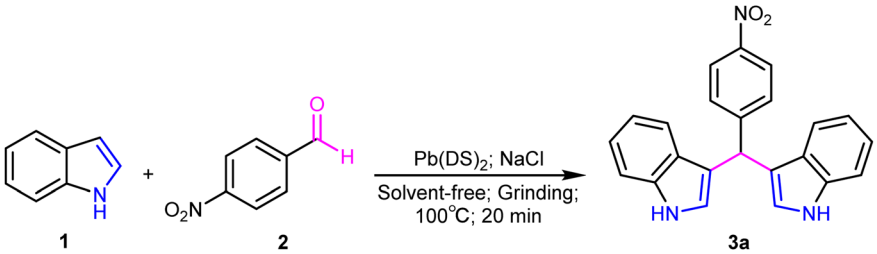

Entry[a]	Catalyst	Carrier[b] (g)	Time (min)	T (°C)	Yield[c] (%)
1			60	rt	N.R.
2		NaCl	30	rt	<1
3		NaCl	30	75	<1
4	$Pb(DS)_2$	NaCl	30	rt	<5
5	$Pb(DS)_2$	NaCl	30	50	15
6	$Pb(DS)_2$	NaCl	30	75	66
7[e]	$Pb(DS)_2$	NaCl	30	100	98
8[e]	$Pb(DS)_2$	NaCl	30	100	98
9[e]	$Pb(DS)_2$	NaCl	30	100	89
10	$Pb(DS)_2$	NaCl	20	100	98
11	$Pb(DS)_2$	NaCl	10	100	73

[a] Reaction conditions: indole **1** (2 mmol; 0.234 g); 4-nitrobenzaldehyde **2** (1 mmol; 0.151 g); $Pb(DS)_2$: lead dodecyl sulfate (0.05 g); 100 °C; solvent-free; solid phase grinding. [b] NaCl: sodium chloride (0.5 g). [c] Heating in an oven for 20 min prior to the ball milling reaction. [d] Isolated yields: all product yields were obtained by column chromatography. [e] The amount of $Pb(DS)_2$ was 0.0625 g; 0.05 g; 0.0375 g; respectively.

284.6 eV, 285.2 eV, and 286.1 eV, corresponding to C–H/C–C, C–C, and C–O bonds, respectively. The high-resolution spectrum of O 1s (Fig. 3b) for the $Pb(DS)_2$ catalyst revealed three main peaks at 532.2 eV, 533.6 eV, and 535.6 eV, attributed to lattice oxygen, –O–S, O═S, and C–O–S bonds. The binding energy of the $Pb(DS)_2$ catalyst at 168.9 eV and 170.0 eV corresponds to the –O–S and –O═S bonds (as shown in Fig. 3c), respectively. In addition, the high-resolution XPS spectra of Pb 4f in the catalyst, primarily composed of the spin–orbit splitting of Pb $4f_{7/2}$ and Pb $4f_{5/2}$, are illustrated in Fig. 3d. For solid-phase grinding synthesized $Pb(DS)_2$ materials, two characteristic peaks located at 139.5 eV and 144.3 eV are assigned to Pb $4f_{7/2}$ and Pb $4f_{3/2}$. This indicates the potential presence of metal Pb(II) ions in the form of oxides.

From a mechanochemical perspective, the recyclability and reusability of metal catalysts are critical factors in their potential industrial application. In order to assess these properties, the reusability of the $Pb(DS)_2$ catalyst was tested in a catalytic model reaction involving *o*-phenylenediamine and benzoyl (as shown in Fig. 4a). After the initial catalytic cycle, the catalyst was readily recovered from the reaction mixture by filtration, washed with ethyl acetate and ethanol (3 × 5 mL), and dried at 45 °C overnight. Subsequently, a new quinoxaline synthesis reaction was conducted using the regenerated catalyst. The results demonstrate that $Pb(DS)_2$ displays exceptional stability in the model catalytic reaction. After eight repeated uses, the target product maintained a yield of 94% with no significant decrease in catalyst activity. In addition, it was observed that the loss of lead and sulfur elements in fresh catalysts and catalysts reused 8 times was approximately 0.11% and 0.13% per cycle, respectively (as shown in Fig. 4a(A)), which efficiently ensured the intrinsic structure and basic composition of the catalyst, and effectively controlled the pollution caused by the loss of toxic substances to the environment. Similarly, the experiment quantitatively analyzed the loss of each catalyst, as shown in Fig. S1.† Quantitative amplification experiments were conducted using a 30-fold equivalent catalyst (detailed experimental methods can be found in the ESI†). It can be seen from S1 that the amount of catalyst used in each cycle experiment shows a decreasing trend. This indicates that mechanical grinding can cause catalyst particles to become finer and more easily lost during repeated use. The cycling stability experiment data (Fig. S1†) reveal a significant law of catalyst mass attenuation: with the increase of the number of cycles, the catalyst feed amount shows a stepwise decreasing feature. This mass loss mainly results from two synergistic mechanisms: first, the particle powdering effect induced by mechanical stress – the shear force generated during the grinding process continuously reduces the particle size of the catalyst, resulting in an increase in specific surface area and surface energy; second, catalyst loss and escape during the operation process, which is specifically manifested as the micro-loss of ultrafine particles during the transfer process. This dual loss mechanism jointly intensifies the irreversible consumption of the catalyst. Therefore, the catalytic effect of the catalyst shows a slight downward trend during the cycling process. However, the ICP characterization results indicated that the loss of lead and sulfur elements remained almost constant in each cycle. The test results showed

Table 2 Synthesis of bis(indolyl)methane derivatives using the $Pb(DS)_2$ catalyst[a]

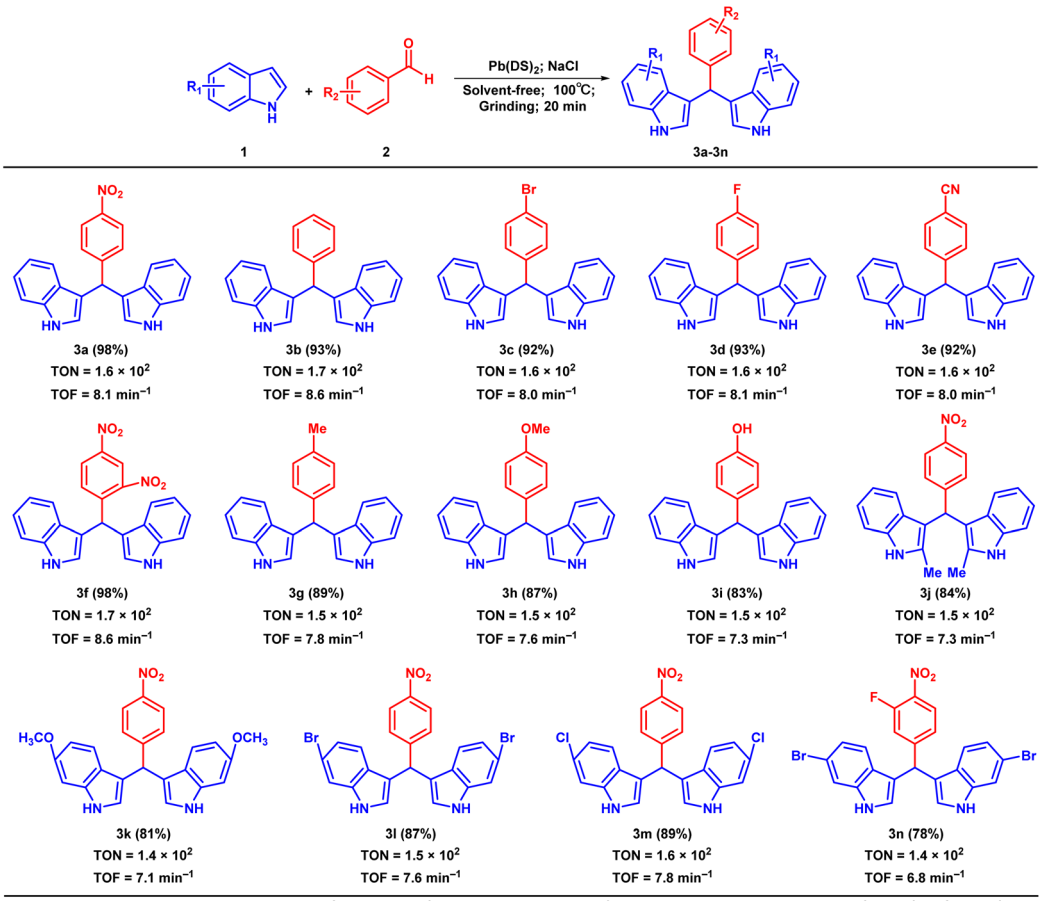

[a] Reaction conditions: **1** (2.0 mmol); **2** (1.0 mmol); $Pb(DS)_2$ (0.05 g); NaCI (0.5 g); heating in an oven for 20 min prior to the ball milling reaction; solvent-free; grinding for 20 min; isolated yields.

that the loss of lead and sulfur elements in the fresh catalyst and after 8 cycles was 0.11% and 0.13%, respectively.

The catalytic and stable performance of catalysts is inherently linked to their stable morphology and internal structure, underscoring the crucial relationship between the structure and activity. The experiment shows that the $Pb(DS)_2$ catalyst has excellent catalytic and cycling performance. In this work, a detailed structural analysis was conducted on the catalyst after eight reuse cycles. Thermal gravimetric analysis (TGA) of all samples over the temperature range of 25–400 °C reveals distinct weight loss trends categorized into three temperature regions, denoted as regions I, II, and III (as depicted in Fig. 4b). The analysis of region I is particularly meaningful, as both the fresh catalyst and the catalyst after 8 repeated cycles experienced weight loss from room temperature to approximately 175 °C, while the raw material SDS appeared from room temperature to approximately 200 °C. This is due to the release of free water molecules upstream of the catalyst surface and the decomposition of low molecular weight compounds. The temperature required for organic catalytic reactions is typically below 175 °C, with the $Pb(DS)_2$ catalyst ensuring structural integrity and catalytic activity within this range. Both fresh and recycled catalysts exhibit excellent thermal stability in this temperature range. It is evident that the loss of the fresh $Pb(DS)_2$ catalyst in region I is 3.3%, while the loss of the catalyst after 8 reuse cycles is 3.1%. It is speculated that the reason may be that the catalyst has undergone repeated mechanical grinding, resulting in a denser structure of the material and a continuous increase in crystallinity, thereby significantly improving its thermal stability. The realization of this special phenomenon is more pronounced in regions II and III. Specifically, between 160 °C and 260 °C (region II), both fresh and recovered catalysts experienced significant weight loss, with loss rates of approximately 52.9% and 36.0%, respectively. Compared with fresh catalysts, catalysts that are reused 8 times have lower quality loss and higher stability characteristics. In region III, ranging from 260 °C to 400 °C, the catalyst undergoes a more moderate loss of around 10%.

The FT-IR analysis showed that the characteristic peak positions of the catalyst remained basically consistent in the fresh state and after 8 cycles (as shown in Fig. 4c). There was a slight change in peak intensity, particularly at 2920 and

Table 3 Synthesis of quinoxaline derivatives using the $Pb(DS)_2$ catalyst[a]

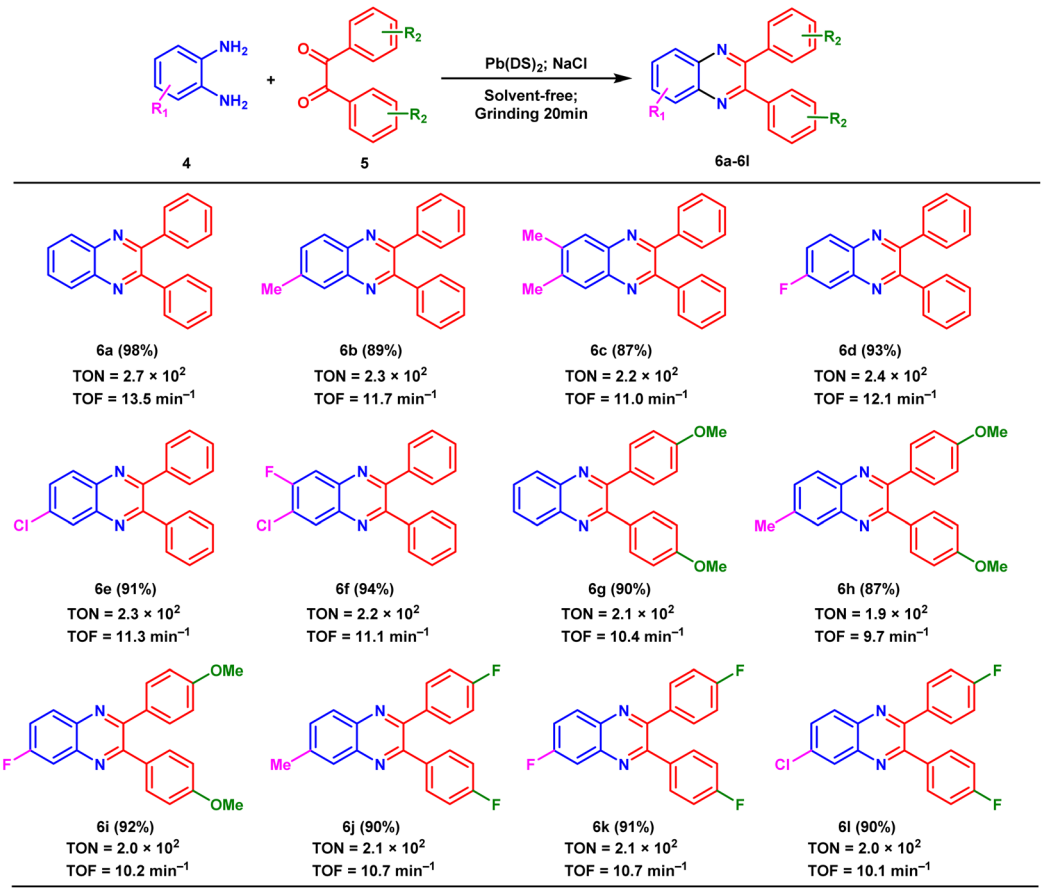

[a] Reaction conditions: **4** (0.5 mmol); **5** (0.5 mmol); $Pb(DS)_2$ (10% wt): NaCl (0 5 g). Preheating for 20 minutes at 75 °C before proceeding with the ball milling reaction; solvent-free; grinding for 20 min; isolated yields.

$2851\ cm^{-1}$. The change in peak intensity also indicates an increase in the crystallinity of the material, which is consistent with the results of TGA analysis. Compared with fresh $Pb(DS)_2$ catalysts, the XRD results of the catalyst after 8 repeated uses exhibited significant differences (as shown in Fig. 4d). The diffraction peak positions of the catalyst have changed after multiple grinding, with the three crystal planes ((001), (002), and (003)) in the spectrum shifting to the right, particularly the (001) crystal plane. This shift indicates a reduction in lattice spacing and a rightward shift in diffraction peak positions due to multiple mechanical grinding. These observations are consistent with previous characterization results, suggesting an improvement in the stability performance of the catalyst after multiple grinding. In addition, the catalyst after 8 repeated uses was characterized and analyzed through other experimental methods, including SEM, TEM, and NMR (as shown in Fig. S1†). The results showed that even after 8 repeated cycles, the catalyst maintained the same nano rod like morphology and characteristics as the original catalyst $Pb(DS)_2$. These research results all demonstrate that the superior catalytic and thermal stability of $Pb(DS)_2$ catalysts can be attributed to the nanorod-like structure of the material. Even after undergoing 8 repeated grinding cycles, the material's nanorod-like structure remains intact. Additionally, the NMR data confirm that the fundamental composition of the material remains unchanged, ensuring the preservation of its inherent properties.

Catalytic performance evaluation of the $Pb(DS)_2$ catalyst

In order to develop an environmentally friendly and energy-saving method for synthesizing biologically important heterocyclic compounds, we prepared the $Pb(DS)_2$ catalyst *in situ* by solvent-free mechanical ball milling. In fact, there have been many reports on this green catalytic method and new catalysts recently, such as the hybridization of C–H and C–N bonds using the CF_2Br_2 catalyst[54] under light conditions. This work employs solvent-free synthesis of nitrogen-containing heterocyclic compounds, including bis(indolyl)methane derivatives and quinoxaline derivatives, all of which involve the reconstruction of C–H and C–N bonds at room temperature.[55] Initially, we selected the synthesis of bis(indolyl)methane derivatives as a model reaction and optimized the reaction conditions using various $Pb(DS)_2$ catalysts and solvent-free grinding. Through rigorous catalyst screening, we identified the optimal

Table 4 Catalytic Biginelli reaction using the $Pb(DS)_2$ catalyst[a]

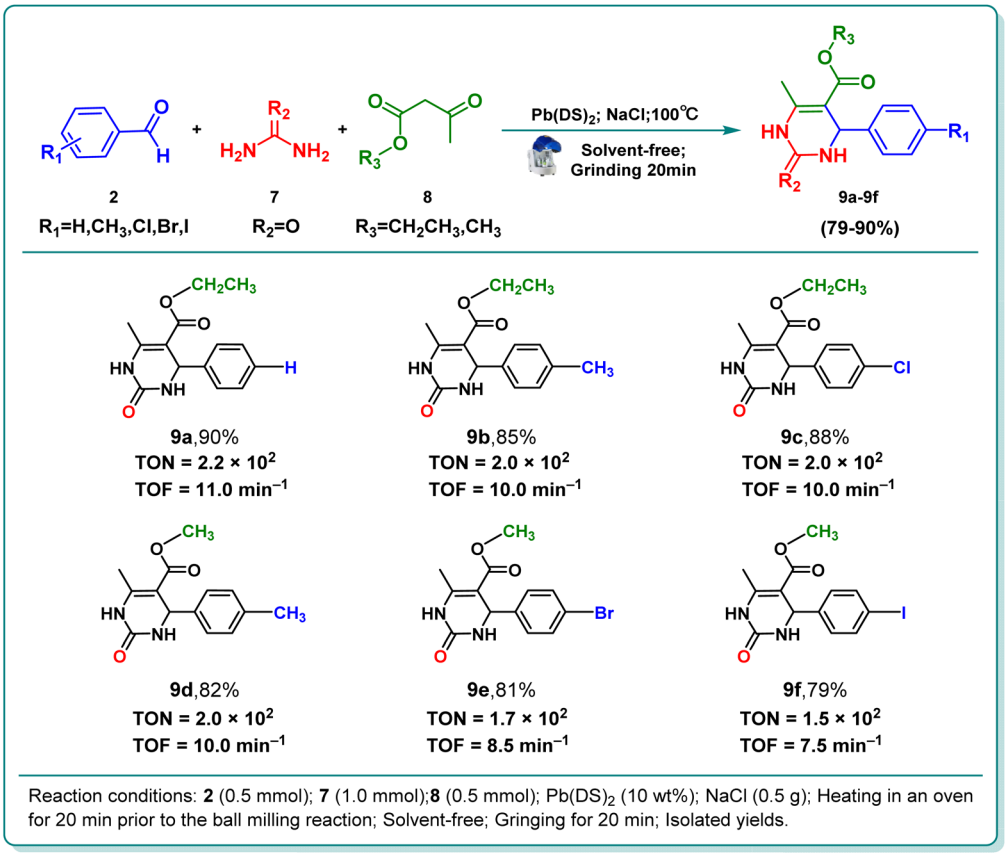

[a] Reaction conditions: **2** (0.5 mmol); **7** (1.0 mmol); **8** (0.5 mmol); $Pb(DS)_2$ (10 wt%); NaCI (0.5 g); heating in an oven for 20 min prior to the ball milling reaction; solvent-free; grinding for 20 min; isolated yields.

conditions for synthesizing compound **3a**, achieving a remarkable 98% product yield with the $Pb(DS)_2$ catalyst, 0.5 g NaCl as a grinding assistant, 20 minutes of grinding time, and 100 °C reaction temperature (Table 1, entry 10).

With the optimized conditions established, we systematically explored the substrate scope for the synthesis of bis(indolyl)methane derivatives by employing a variety of aldehydes and indoles, as summarized in Table 2. To our delight, compounds bearing a wide range of substituents were obtained with good to excellent yields (Table 2, **3a–3n**). We investigated the reaction between indole and benzaldehyde with different substituent groups to expand the universality of substrates (**3a–3i**). It is apparent that the electron withdrawing groups of the benzaldehyde compounds achieved better yields in a shorter time (**3a–3f**) when compared with their electron donating groups (**3g–3i**). Compound **3n** was synthesized for the first time with a target yield of 78%. Furthermore, we extended our investigation to the reaction between 4-nitrobenzaldehyde and indole compounds with different substituents to further broaden the range of substrates. The results have demonstrated excellent production of the target product in a short period of time (**3j–3m**). In addition, all synthesized compounds were obtained by calculating their TON and TOF values.

The newly developed nanorod $Pb(DS)_2$ catalyst was employed in the synthesis of nitrogen-containing heterocyclic compounds through mechanical ball milling, aiming to validate its efficacy for organic catalytic reactions. $Pb(DS)_2$ demonstrated exceptional performance in the model reaction (the optimization of reaction conditions is shown in Table. S1†), and it was applied to hydrogen transfer reactions involving *o*-phenylenediamine and various benzoyl compounds with different substituents under optimized conditions (as shown in Table 3). This result illustrates the hydrogen transfer reaction between benzoyl and different aromatic 1,2-diamine compounds (**6a–6f**). Notably, both electron donating and electron withdrawing groups in aromatic 1,2-diamines were found to be compatible with benzoyl groups, underscoring the robustness of the $Pb(DS)_2$ catalyst in the reaction system. Particularly, the reaction between *o*-phenylenediamine and benzoyl yielded an impressive 98% yield (**6a**), while other products achieved target yields exceeding 87% (**6b–6f**). Similarly, reactions involving 1,2-diketone substituted with bis(4-methoxy) and *o*-phenylenediamine with various substituents resulted in target product yields of 90% (**6g**), 87% (**6h**), and 92% (**6i**), respectively. Specifically, the reaction of 1,2-diketones substituted with bis(4-fluoro) and *o*-phenylenediamine with various substituents resulted in high

Table 5 Comparison of different methods for catalytic synthesis of bis(indolyl)methane derivatives

Entry	Catalysts	Conditions	Time	Yield
1	$Fe(DS)_3$	Water, R.T.	5 h	97 (ref. 62)
2	PANF-PAMSA	Water, R.T.	4 h	95 (ref. 63)
3	DBSA	Water, 40 °C	1 h	90 (ref. 64)
4	PPL	Water, 50 °C	72 h	98 (ref. 65)
5	Itaconic acid	Water, 100 °C	45 min	95 (ref. 66)
6	Amberlyst	MeCN, R.T.	6 h	98 (ref. 67)
7	$BF_3 \cdot Et_2O$	Et_2O, R.T.	2 h	93 (ref. 68)
8	$Al(DS)_3$	H_2O : EtOH (2 : 1), R.T.	4 h	89 (ref. 69)
9	$Sr(DS)_2$	H_2O : EtOH (2 : 1), R.T.	12 h	90 (ref. 69)
10	I_2	EtOH, 40 °C	24 h	96 (ref. 70)
11	Bu_4NHSO_4	EtOAc, 60 °C	1 h	90 (ref. 71)
12	$FePO_4$	Glycerol, 75 °C	5 h	84 (ref. 72)
13	DAHP	Solvent-free, 80 °C	2 h	89 (ref. 73)
14	$MgAl_2O_4$	Solvent-free, 100 °C	2 h	54 (ref. 74)
15	$La(DS)_3$	Solvent-free, 50 °C	30 min	96 (ref. 46)
This work	$Pb(DS)_2$	Solvent-free, 100 °C	20 min	98

product yields exceeding 90% (**6j–6l**), regardless of steric hindrance. These compounds, containing abundant fluorine substituent groups, may exhibit advantageous biological activities. Similarly, TON and TOF values were calculated for all compounds.

Multicomponent reactions can synthesize more than two repeated products in one step, enabling the formation of the desired product in the shortest time and the most efficient way. These reactions are atomically and energetically economical compared to linear synthesis. These reactions have the advantages of short reaction times, high yields, cost-effectiveness, and less waste generation. In addition, it can be said that almost all reactants are involved in the production of the product without the need to separate the intermediates, which is actually in line with the principles of green chemistry.[56,57] Heterocyclic compounds are considered as important structural units in many drugs and bioactive molecules, and have a wide range of important applications in human life and various industrial and biological fields.[58–60] Nitrogenous and oxygenic rings are the two most important classes of this class of compounds, and they are widely found in the skeletons of drugs and bioactive materials.[58,61] The Biginelli reaction, a multi-component organic reaction that involves the formation of C–C and C–N bonds, is an effective way to synthesize multifunctional heterocyclic compounds and one of the most influential multicomponent reactions.[58] Building on the successful use of the $Pb(DS)_2$ catalyst in previous reactions, we sought to broaden the scope of catalytic reactions by exploring a three-component Biginelli reaction. Through this approach, we were able to synthesize six target products with yields ranging from 79% to 90% in a short timeframe (**9a–9f**), as illustrated in Table 4. These results demonstrate that the $Pb(DS)_2$ catalyst is effective in facilitating multi-component reactions, highlighting its catalytic prowess. This study unveils a novel pathway for the environmentally friendly synthesis of heterocyclic bioactive

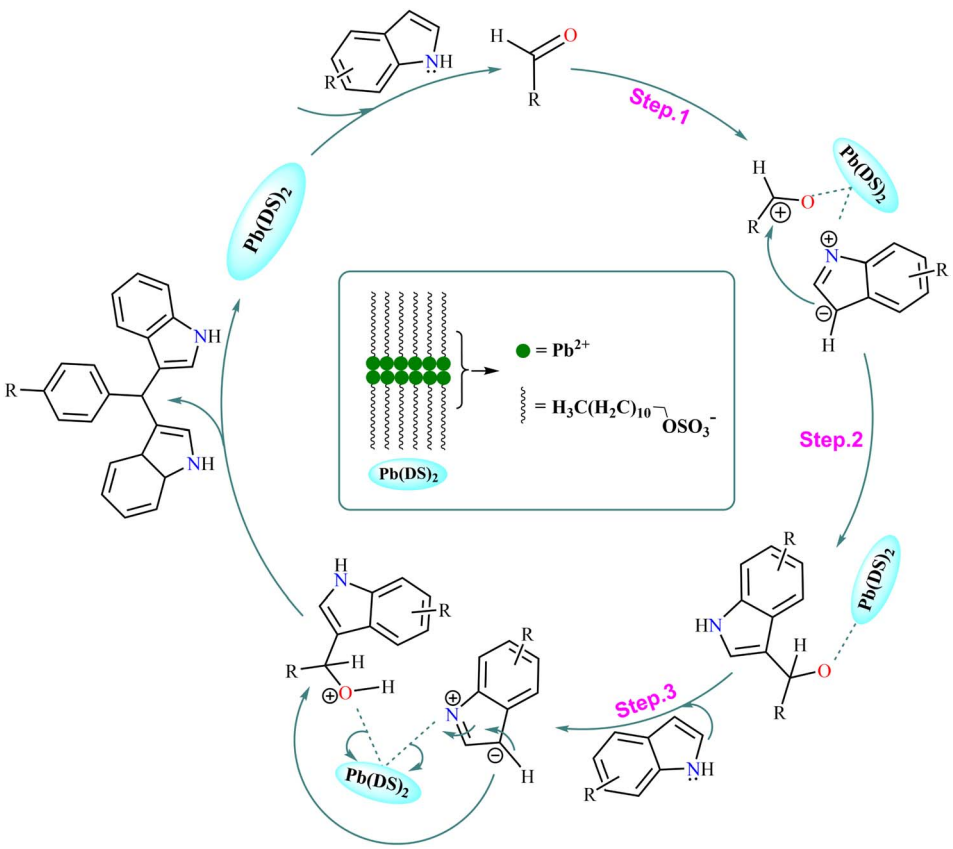

Fig. 5 The speculated mechanism of the $Pb(DS)_2$ catalyzed indole methylation reaction.

organic molecules. Future research by our team will delve further into this promising area of investigation.

In addition, this work systematically compared the synthesis of bis(indolyl)methane derivatives using other series of catalyst materials. Compared with other catalysts reported in the literature, the $Pb(DS)_2$ catalyst material exhibits advantages such as a simple preparation method, short reaction time, no requirement for organic solvents, and high catalytic efficiency. The $Pb(DS)_2$ catalyst maintained its activity over 8 consecutive reuse cycles without a significant decrease in activity (Table 5).

Based on the aforementioned analysis, we speculate to provide a mechanism for the $Pb(DS)_2$ catalyzed indole methylation reaction (as shown in Fig. 5), which is consistent with the typical proton acid catalyzed reaction mechanism.[46,75] The catalyst activates the carbonyl group in aromatic aldehydes, then reacts with indole, followed by dehydration to eliminate water molecules, ultimately producing bis(indolyl)methane derivatives.

Conclusion

The $Pb(DS)_2$ catalyst with uniform size nanorod structure was successfully prepared by a mechanical chemical ball milling method, showing good catalytic activity and stability. The catalyst enabled highly efficient solvent-free synthesis of heterocyclic derivatives, such as bis(indolyl)methane derivatives (78–98%) and quinoxaline derivatives (87–98%) in 20 minutes. In addition, the $Pb(DS)_2$ catalyst has also demonstrated excellent catalytic performance in the Biginelli reaction. Elemental analysis showed that there was no significant change in the composition and content of the elements in the catalyst, which effectively maintained the activity and stability of the catalyst. Especially the loss of lead element can minimize environmental pollution to the greatest extent possible (the loss of Pb element in the catalyst is about 0.11% per cycle). In conclusion, the $Pb(DS)_2$ catalytic material presented in this study exhibits a simple preparation method, excellent catalytic performance, wide reaction versatility, and long cycle life. With the development of mechanochemical research, this kind of catalyst system is expected to be widely used in various solvent-free mechanochemical reactions.

Experimental section

Materials

All reagents were purchased from Shanghai Titan Co., Ltd and Aladdin Reagent Co., Ltd. All reagents and drugs were of analytical grade (AR).

Preparation method of the $Pb(DS)_2$ catalyst

First, lead nitrate ($Pb(NO_3)_2$; 1.0 mmol; 0.331 g) and sodium dodecyl sulfate (SDS; 2.0 mmol; 0.577 g) were weighed in a specific ratio and combined with stainless steel grinding balls (diameter: 5 mm (with 6 additions) and 8 mm (with 3 additions), volume ratio 1 : 4) in a planetary ball mill jar (ball powder mass ratio of 10 : 1), and then subjected to continuous ball milling at 600 rpm for 30 minutes. Upon completion of the reaction, the resulting mixture was transferred to a beaker, dissolved in distilled water, stirred, and washed. The white precipitate obtained was filtered using a sand core funnel, washed with a small amount of distilled water until neutral (3 × 5 mL), and the white solid product was collected. Subsequently, the product was dried in a vacuum drying oven at 45 °C for 24 hours to yield the final white solid powder, identified as $Pb(DS)_2$. Further experimental details can be found in the ESI.†

Data availability

All relevant data are within the paper.

Conflicts of interest

There are no conflicts to declare.

Acknowledgements

This work was financially supported by the Inner Mongolia Autonomous Region Alxa League Science and Technology Plan Project (AMKJ2023-12); the National College Students' Innovation and Entrepreneurship Training Program Project (G20241075304); the Ningxia Hui Autonomous Region High Level Teaching Reform Project (bjg2023073) the Ningxia Natural Science Foundation Project (2024AAC03314, 2024AAC05071) and 2024 Science and Technology Plan Project of Guyuan City (2024BGTYF01-41).

References

1 X. Liu, Y. Li, L. Zeng, X. Li, N. Chen, S. Bai, H. He, Q. Wang and C. Zhang, A review on mechanochemistry: Approaching advanced energy materials with greener force, *Adv. Mater.*, 2022, **34**(46), 2108327.
2 K. J. Ardila-Fierro and J. G. Hernández, Sustainability assessment of mechanochemistry by using the twelve principles of green chemistry, *ChemSusChem*, 2021, **14**(10), 2145–2162.
3 N. Fantozzi, J.-N. Volle, A. Porcheddu, D. Virieux, F. García and E. Colacino, Green metrics in mechanochemistry, *Chem. Soc. Rev.*, 2023, **52**, 6680–6714.
4 V. Štrukil, Mechanochemical organic synthesis: The art of making chemistry green, *Synlett*, 2018, **29**(10), 1281–1288.
5 J. L. Do and T. Friščić, Mechanochemistry: a force of synthesis, *ACS Cent. Sci.*, 2017, **3**(1), 13–19.
6 T. Friščić, C. Mottillo and H. M. Titi, Mechanochemistry for synthesis, *Angew. Chem., Int. Ed.*, 2020, **132**(3), 1030–1041.
7 G.-W. Wang, Mechanochemical organic synthesis, *Chem. Soc. Rev.*, 2013, **42**(18), 7668–7700.
8 D. Tan and T. Friščić, Mechanochemistry for organic chemists: An update, *Eur. J. Org Chem.*, 2018, **1**, 18–33.
9 G.-W. Wang and J. Gao, Solvent-free bromination reactions with sodium bromide and oxone promoted by mechanical milling, *Green Chem.*, 2012, **14**(4), 1125–1131.

10 E. Torabi, A. Abdar, N. Lotfian, M. Bazargan, C. Simms, M. A. Moussawi and T. N. Parac-Vogt, Advanced materials in sorbent-based analytical sample preparation, *Coord. Chem. Rev.*, 2024, **506**, 215680.
11 A. Abdar, A. Amiri and M. Mirzaei, Electrospun mesh pattern of polyvinyl alcohol/zirconium-based metal-organic framework nanocomposite as a sorbent for extraction of phthalate esters, *J. Chromatogr. A*, 2023, **1707**, 464295.
12 M. Nazari, A. S. Saljooghi, M. Ramezani, M. Alibolandi and M. Mirzaei, Current status and future prospects of nanoscale metal–organic frameworks in bioimaging, *J. Mater. Chem. B*, 2022, **10**(43), 8824–8851.
13 X. He, Z. Jiang, O. U. Akakuru, J. Li and A. Wu, Nanoscale covalent organic frameworks: from controlled synthesis to cancer therapy, *Chem. Commun.*, 2021, **57**(93), 12417–12435.
14 L. Yang, Z. Pan and Z. Tian, Mechanochemical Synthesis of Solid Catalysts and Application in Catalytic Reaction, *ChemCatChem*, 2024, **16**(10), e202301519.
15 S. Niyazi, B. Pouramiri and K. Rabiei, Functionalized nanoclinoptilote as a novel and green catalyst for the synthesis of Mannich bases derived from 4-hydroxy coumarin, *J. Mol. Struct.*, 2022, **1250**, 131908.
16 K. Rabiei, Z. Mohammadkhani, H. Keypour and J. Kouhdareh, Palladium Schiff base complex-modified Cu(BDC-NH_2) metal–organic frameworks for C-N coupling, *RSC Adv.*, 2023, **13**(12), 8114–8129.
17 H. Naeimi, K. Rabiei and F. Salimi, Template synthesis of some double Schiff-base metal (II) complexes through one pot four component reactions under mild and convenient conditions, *J. Coord. Chem.*, 2009, **62**(7), 1199–1205.
18 F. Xie, M. Zhang, H. Jiang, M. Chen, W. Lv, A. Zheng and X. Jian, Efficient synthesis of quinoxalines from 2-nitroanilines and vicinal diols via a ruthenium-catalyzed hydrogen transfer strategy, *Green Chem.*, 2015, **17**(1), 279–284.
19 G. C. Nandi, S. Samai, R. Kumar and M. S. Singh, Silica-gel-catalyzed efficient synthesis of quinoxaline derivatives under solvent-free conditions, *Synth. Commun.*, 2011, **41**(3), 417–425.
20 P. Yang, C. Zhang, W. C. Gao, Y. Ma, X. Wang, L. Zhang, J. Yue and B. Tang, Nickel-catalyzed borrowing hydrogen annulations: access to diversified N-heterocycles, *Chem. Commun.*, 2019, **55**(54), 7844–7847.
21 C. Zhang, Z. Zhang, D. Wang, W. Wang, B. Jin, T. Wen, L. Ye, Z. N. Chen and H. Cai, DMSO/^{t}BuONa/O_2-mediated efficient syntheses of diverse quinoxalines through α-imino radicals, *Chem. Commun.*, 2023, **59**(35), 5217–5220.
22 A. Sharma, R. Dixit, S. Sharma, S. Dutta, S. Yadav, B. Arora, M. B. Gawande and R. K. Sharma, Efficient and sustainable Co_3O_4 nanocages based nickel catalyst: A suitable platform for the synthesis of quinoxaline derivatives, *Mol. Catal.*, 2021, **504**, 111454.
23 H. Veisi, R. Gholbedaghi, J. Malakootikhah, A. Sedrpoushan, B. Maleki and D. Kordestani, Trichloroisocyanuric acid-catalyzed reaction of indoles: An expeditious synthesis of bis-indolyl, tris-indolyl, di (bis-indolyl), tri (bis-indolyl), and tetra (bis-indolyl) methane under solid-state conditions, *J. Heterocycl. Chem.*, 2010, **47**(6), 1398–1405.
24 S. Bhargava, P. Soni and D. Rathore, An environmentally benign attribute for the expeditious synthesis of quinoxaline and its derivatives, *J. Mol. Struct.*, 2019, **1198**, 126758.
25 A. A. Sosa, V. Palermo, P. Langer, R. Luque, G. P. Romanelli and L. R. Pizzio, Tungstophosphoric acid/mesoporous silicas as suitable catalysts in quinoxaline synthesis, *Mol. Catal.*, 2022, **517**, 112046.
26 G. Jagannivasan, G. N. Nair and S. Haridas, Visible light-assisted $H_4[PW_{11}VO_{40}]$ catalysed synthesis of bis(indolyl) methanes, *Mol. Catal.*, 2023, **547**, 113285.
27 S. Nagayama and S. Kobayashi, A novel chiral lead (II) catalyst for enantioselective aldol reactions in aqueous media, *J. Am. Chem. Soc.*, 2000, **122**(46), 11531–11532.
28 M. S. Akanni, H. D. Burrows, H. A. Ellis and I. E. Ozowara, The thermal behaviour of basic lead (II)dodecylsulphate, *Thermochim. Acta*, 1982, **59**(1), 19–23.
29 M. Ghaedi, H. Tavallali, A. Shokrollahi, M. Zahedi, M. Montazerozohori and M. Soylak, Flame atomic absorption spectrometric determination of zinc, nickel, iron and lead in different matrixes after solid phase extraction on sodium dodecyl sulfate (SDS)-coated alumina as their bis (2-hydroxyacetophenone)-1, 3-propanediimine chelates, *J. Hazard. Mater.*, 2009, **166**, 1441–1448.
30 P. Ma, Y. Hou, Z. Chen, J. Su, L. Li, N. Liu, Z. Zhang, X. Jiang, F. Long, Y. Ma and Y. Gao, Enhanced stability of $CsPbBr_3$ Quantum Dots by anchoring on the hierarchical three-dimensional layered double hydroxide, *Chem. Eng. J.*, 2021, **425**, 130471.
31 M. T. Hoang, C. Han, Z. Ma, X. Mao, Y. Yang, S. S. Madani, P. Shaw, Y. Yang, L. Peng, C. Y. Toe, J. Pan, R. Amal, A. Du, T. Tesfamichael, Z. Han and H. Wang, Efficient CO_2 reduction to formate on $CsPbI_3$ nanocrystals wrapped with reduced graphene oxide, *Nano-Micro Lett.*, 2023, **15**, 161.
32 J. Yin, X. Song, C. Sun, Y. Jiang, Y. He and H. Fei, Modular Inorganic Dimensionality of Unstable Lead Halide Coordination Polymers for Photocatalytic CO_2 Reduction to Ethanol, *Angew. Chem., Int. Ed.*, 2024, **63**(16), e202316080.
33 X. Chen, C. Peng, W. Dan, L. Yu, Y. Wu and H. Fei, Bromo- and iodo-bridged building units in metal organic frameworks for enhanced carrier transport and CO_2 photoreduction by water vapor, *Nat. Commun.*, 2022, **13**, 4592.
34 R. Ghiai, S. Alavinia, R. Ghorbani-Vaghei, A. Khazaei, R. Karimi-Nami and I. Karakaya, Synthesis of benzothiazoles using an iron-anchored polysulfonamide modified layered double oxide/sodium alginate nanocomposite, *J. Mater. Chem. A*, 2024, **12**(9), 5474–5492.
35 K. Manabe, Y. Mori, T. Wakabayashi, S. Nagayama and S. Kobayashi, Organic synthesis inside particles in water: lewis acid-surfactant-combined catalysts for organic reactions in water using colloidal dispersions as reaction media, *J. Am. Chem. Soc.*, 2000, **122**(30), 7202–7207.
36 K. Manabe, S. Iimura, X. M. Sun and S. Kobayashi, Dehydration reactions in water. Brønsted acid-surfactant-

combined catalyst for ester, ether, thioether, and dithioacetal formation in water, *J. Am. Chem. Soc.*, 2002, **124**(40), 11971–11978.

37 K. Masuda and S. Kobayashi, Direct and quantitative monitoring of catalytic organic reactions under heterogeneous conditions using direct analysis in real time mass spectrometry, *Chem. Sci.*, 2020, **11**(19), 5105–5112.

38 T. Kitanosono, P. Xu and S. Kobayashi, Chiral Lewis acids integrated with single-walled carbon nanotubes for asymmetric catalysis in water, *Science*, 2018, **362**(6412), 311–315.

39 R. Singh, D. Bhardwaj, S. A. Ganaie and A. Singh, Lewis acid surfactant combined (LASC) catalyst as a versatile heterogeneous catalyst in various organic transformations, Mini-Rev, *Org. Chem.*, 2020, **17**(2), 124–140.

40 L. Zhang and J. Wu, Friedlnder synthesis of quinolines using a Lewis acid-surfactant-combined catalyst in water, *Adv. Synth. Catal.*, 2007, **349**(7), 1047–1051.

41 M. A. Zolfigol, P. Salehi, M. Shiri and Z. Tanbakouchian, A new catalytic method for the preparation of bis-indolyl and tris-indolyl methanes in aqueous media, *Catal. Commun.*, 2007, **8**(2), 173–178.

42 H. R. Safaei, M. Shekouhy, S. Khademi, V. Rahmanian and M. Safaei, Diversity-oriented synthesis of quinazoline derivatives using zirconium tetrakis(dodecylsulfate) [$Zr(DS)_4$] as a reusable Lewis acid-surfactant-combined catalyst in tap water, *J. Ind. Eng. Chem.*, 2014, **20**(5), 3019–3024.

43 M. Lafantaisie, A. Mirabaud, B. Plancq and T. Ollevier, Iron(II)-derived Lewis acid/surfactant combined catalysis for the enantioselective mukaiyama aldol reaction in pure water, *ChemCatChem*, 2014, **6**(8), 2244–2247.

44 R. Singh and S. A. Ganaie, An efficient synthesis of quinaxoline derivatives using $Fe(DS)_3$ as a lewis acid-surfactant-combined catalyst, *Chem. Sci. Trans.*, 2016, **5**(3), 603–610.

45 H. Veisi, B. Maleki, F. H. Eshbala, H. Veisi, R. Masti, S. S. Ashrafib and M. Baghayeri, In situ generation of Iron (III) dodecyl sulfate as Lewis acid-surfactant catalyst for synthesis of bis-indolyl, tris-indolyl, Di(bis-indolyl), Tri(bis-indolyl), tetra (bis-indolyl)methanes and 3-alkylated indole compounds in water, *RSC Adv.*, 2014, **4**(58), 30683–30688.

46 Z. Wu, X. Li, P. Jiang, G. Feng, L. A. Cao, X. M. Wang and E. Feng, Mechanical milling promotes the preparation of catalyst lanthanum dodecyl sulfate and green solvent-free grinding for synthesis of N-heterocyclic derivatives, *Appl. Catal., A*, 2024, **684**, 119893.

47 J. Kang, G. Liu, Q. Hu, Y. Huang, L. M. Liu, L. Dong and L. Guo, Parallel nanosheet arrays for industrial oxygen production, *J. Am. Chem. Soc.*, 2023, **145**(46), 25143–25149.

48 G. F. Ghesti, J. L. de Macedo, V. C. I. Parente, J. A. Dias and S. C. L. Dias, Synthesis, characterization and reactivity of Lewis acid/surfactant cerium trisdodecylsulfate catalyst for transesterification and esterification reactions, *Appl. Catal., A*, 2009, **335**(1–2), 139–147.

49 V. B. Kartha, L. C. Leitch and H. H. Mantsch, Infrared and Raman spectra of alkali palmityl sulfates, *Can. J. Chem.*, 1984, **62**(1), 128–132.

50 M. Machida, K. Kawamura, T. Kawano, D. Zhang and K. Ikeue, Layered Pr-dodecyl sulfate mesophases as precursors of $Pr_2O_2SO_4$ having a large oxygen-storage capacity, *J. Mater. Chem.*, 2006, **16**(30), 3084–3090.

51 L. Sicard, P. L. Llewellyn, J. Patarin and F. Kolenda, Investigation of the mechanism of the surfactant removal from a mesoporous alumina prepared in the presence of sodium dodecylsulfate, *Microporous Mesoporous Mater.*, 2001, **44**, 195–201.

52 J. A. Poston Jr, R. V. Siriwardanea, E. P. Fishera and A. L. Miltz, Thermal decomposition of the rare earth sulfates of cerium (III), cerium (IV), lanthanum (III) and samarium (III), *Appl. Surf. Sci.*, 2003, **214**(1–4), 83–102.

53 R. P. Sperline, Infrared spectroscopic study of the crystalline phases of sodium dodecyl sulfate, *Langmuir*, 1997, **13**(14), 3715–3726.

54 W. Zuo, L. Zuo, X. Geng, Z. Li and L. Wang, Radical-polar crossover enabled triple cleavage of CF_2Br_2: a multicomponent tandem cyclization to 3-fluoropyrazoles, *Org. Lett.*, 2023, **25**(32), 6062–6066.

55 W. Zuo, L. Zuo, X. Geng, Z. Li and L. Wang, Photoinduced C–H heteroarylation of enamines via quadruple cleavage of CF_2Br_2, *Org. Chem. Front.*, 2023, **10**(24), 6112–6116.

56 R. V. Patil, J. U. Chavan, D. S. Dalal, V. S. Shinde and A. G. Beldar, Biginelli reaction: Polymer supported catalytic approaches, *ACS Comb. Sci.*, 2019, **21**(3), 105–148.

57 S. Habibzadeh, G. Firouzzadeh Pasha, M. Tajbakhsh, N. Amiri Andi and E. Alaee, A novel ternary GO@SiO_2-HPW nanocomposite as an efficient heterogeneous catalyst for the synthesis of benzazoles in aqueous media, *J. Chin. Chem. Soc.*, 2019, **66**(8), 934–944.

58 X. H. Chen, X. Y. Xu, H. Liu, L. F. Cun and L. Z. Gong, Highly enantioselective organocatalytic Biginelli reaction, *J. Am. Chem. Soc.*, 2006, **128**(46), 14802–14803.

59 B. Maleki, M. Chahkandi, R. Tayebee, S. Kahrobaei, H. Alinezhad and S. Hemmati, Synthesis and characterization of nanocrystalline hydroxyapatite and its catalytic behavior towards synthesis of 3, 4-disubstituted isoxazole-5(4H)-ones in water, *Appl. Organomet. Chem.*, 2019, **33**(10), e5118.

60 M. Keshvari Kenari, S. Asghari, B. Maleki and M. Mohseni, Preparation of nanomagnetic alginate modified by histidine as an antibacterial agent and a reusable green catalyst for the three-component synthesis of 2-amino-4H-chromenes and tetrahydropyrimidines, *Res. Chem. Intermed.*, 2024, **50**(2), 905–924.

61 S. S. Karbasaki, G. Bagherzade, B. Maleki and M. Ghani, Fabrication of sulfamic acid functionalized magnetic nanoparticles with denderimeric linkers and its application for microextraction purposes, one-pot preparation of pyrans pigments and removal of malachite green, *J. Taiwan Inst. Chem. Eng.*, 2021, **118**, 342–354.

62 S. Y. Wang and S. J. Ji, Facile synthesis of bis (indolyl) methanes catalyzed by ferric dodecyl sulfonate [$Fe(DS)_3$] in

water at room temperature, *Synth. Commun.*, 2008, **38**(8), 1291–1298.

63 X. L. Shi, X. Xing, H. Lin and W. Zhang, Synthesis of Polyacrylonitrile Fiber-Supported Poly (ammonium methanesulfonate)s as Active and Recyclable Heterogeneous Brønsted Acid Catalysts, *Adv. Synth. Catal.*, 2014, **356**(10), 2349–2354.

64 B. Pawar, V. Shinde and A. Chaskar, n-Dodecylbenzene Sulfonic Acid (DBSA) as a Novel Brønsted Acid Catalyst for the Synthesis of Bis (indolyl) methanes and Bis (4-hydroxycoumarin-3-yl) methanes in Water, *Green Sustainable Chem.*, 2013, **3**, 56–60.

65 Z. Xiang, Z. Liu, X. Chen, Q. Wu and X. Lin, Biocatalysts for cascade reaction: porcine pancreas lipase (PPL)-catalyzed synthesis of bis (indolyl) alkanes, Amino, *Acids*, 2013, **45**, 937–945.

66 S. B. Kasar and S. R. Thopate, Synthesis of bis (indolyl) methanes using naturally occurring, biodegradable itaconic acid as a green and reusable catalyst, *Curr. Org. Synth.*, 2018, **15**(1), 110–115.

67 B. Ke, Y. Qin, Y. Wang and F. Wang, Amberlyst-Catalyzed Reaction of Indole: Synthesis of Bisindolylalkane, *Synth. Commun.*, 2005, **35**(9), 1209–1212.

68 X. F. Xu, Y. Xiong, X. G. Ling, X. M. Xie, J. Yuan, S. T. Zhang and Z. R. Song, A practical synthesis of bis (indolyl) methanes catalyzed by $BF_3 \cdot Et_2O$, *Chin. Chem. Lett.*, 2014, **25**(3), 406–410.

69 M. A. Zolfigol, P. Salehi, M. Shiri and Z. Tanbakouchian, A new catalytic method for the preparation of bis-indolyl and tris-indolyl methanes in aqueous media, *Catal. Commun.*, 2007, **8**(2), 173–178.

70 X. Y. Zhou and X. Chen, Halogen Bond-Catalyzed Friedel-Crafts Alkylation of Indole with Ketones and Aldehydes for the Synthesis of Symmetrical 3, 3'-diindolylmethanes Using Simple Halogen Donor Catalyst, *Lett. Org. Chem.*, 2021, **18**(8), 604–610.

71 S. H. Siadatifard, M. Abdoli-Senejani and M. A. Bodaghifard, An efficient method for synthesis of bis (indolyl) methane and di-bis (indolyl) methane derivatives in environmentally benign conditions using TBAHS, *Cogent Chem.*, 2016, **2**(1), 1188435.

72 K. F. Behbahani and M. Sasani, Facile synthesis of bis (indolyl) methanes using iron (III) phosphate, *J. Serb. Chem. Soc.*, 2012, **77**(9), 1157–1163.

73 M. Dabiri, P. Salehi, M. Baghbanzadeh, Y. Vakilzadeh and S. Kiani, Diammonium hydrogen phosphate as an efficient and inexpensive catalyst for the synthesis of bis (indolyl) methanes under solvent-free conditions, *Monatsh. Chem.*, 2007, **138**, 595–597.

74 K. Nikoofar, M. Haghighi and Z. Khademi, Preparation, characterization, and catalytic application of metallic nanocrystalline $MgAl_2O_4$ in the synthesis of 3-hydroxy-3-indolyl-indolin-2-ones, symmetrical and unsymmetrical 3, 3'-bis (indolyl) indolin-2-ones, and 3, 3′-bis (indolyl) methanes, *Arabian J. Chem.*, 2019, **12**(8), 3776–3784.

75 Z. Wu, G. Wang, Z. Li, E. Feng, Y. Liang, H. Zhan and W. Liu, Solvent-free multi-component synthesis of unsymmetrical bis (indolyl) alkanes with Lewis acid-surfactant-SiO_2 as nanocatalyst, *Synth. Commun.*, 2021, **51**(8), 1206–1217.